International Journal of Heat and Mass Transfer 98 (2016) 631–642

Contents lists available at ScienceDirect

International Journal of Heat and Mass Transfer

journal homepage: www.elsevier.com/locate/ijhmt

Experimental study of boiling heat transfer in smooth/micro-fin tubes of four refrigerants

G.B. Jiang [a], J.T. Tan [b], Q.X. Nian [a], S.C. Tang [a], W.Q. Tao [a,*]

[a] Key Laboratory of Thermo-Fluid Science and Engineering of MOE, School of Energy and Power Engineering, Xi'an Jiaotong University, Xi'an, Shaanxi 710049, China
[b] Key Laboratory of Electronic Materials Research Laboratory of MOE, School of Electronic and Information Engineering, Xi'an Jiaotong University, Xi'an, Shaanxi 710049, China

ARTICLE INFO

Article history:
Received 26 October 2015
Received in revised form 2 March 2016
Accepted 6 March 2016
Available online 31 March 2016

Keywords:
Micro-fin tubes
Boiling
Heat transfer coefficient
Pressure drop

ABSTRACT

An experimental investigation of boiling characteristics in a horizontal smooth and micro-fin tube with 9.52 mm outside diameter and 1 m length was conducted. The refrigerants tested were R22, R134a, R407C and R410A while vapour quality ranges from 0.1 to 0.9, mass flux 50, 250, 450 kg m^{-2} s^{-1} and heat flux of 5, 12.5, 20 kW m^{-2}. The saturation temperature is 5 °C. For the smooth tube, the average heat transfer coefficients of R134a, R407C and R410A are 110.9%, 78.0% and 125.2% of those of R22 in test conditions respectively. For the micro-fin tube, the average heat transfer coefficients of R22, R134a, R407C and R410A are 1.86, 1.80, 1.69 and 1.78 times higher than those of the smooth tube. The pressure drop of R22, R407C and R410A for the smooth tube is similar to each other while the pressure drop of R134a is 1.7 times higher. The average pressure drop of R22, R134a, R407C and R410A for the micro-fin tube is 1.42, 1.30, 1.45 and 1.40 times higher when compared with that for the smooth one. Considering the effect of heat transfer enhancement and pressure drop augment, the efficiency index η_1 which values the thermo-hydraulic performance at identical flow rate of R22, R134a, R407C and R410A in the micro-fin tube used is 1.31, 1.38, 1.17 and 1.27 respectively compared with the smooth tube.

1. Introduction

Micro-fin tubes are characterized by high heat transfer coefficients, low pressure drop penalty, less material consumption in manufacturing and reduction of refrigerant charge. Due to these excellent advantages, micro-fin tubes are widely used in residential air-conditioners and automobile cooling systems. Since the development of micro-fin tubes for improving the heat transfer coefficient in evaporators and condensers in refrigeration applications started by Hitachi, Ltd in 1977 [1], a number of researches have been conducted to improve the performance of micro-fin tubes by changing geometric parameters like fin number, fin height, fin angle and helical angle. Some typical results are reported in [2–5].

In order to protect environment, various R22 alternatives are now used in refrigeration applications. There are many literatures on the performance of heat transfer coefficients and pressure drop in flow condensation and boiling [2–23]. Some correlations of R22 and its alternatives have been obtained in recent years [18–23].

Schlager et al. [2] studied evaporation and condensation heat transfer coefficients of R22 in three micro-fin tubes. The mass fluxes were from 150 to 500 kg m^{-2} s^{-1} while the saturation temperature was from 273 to 278 K for evaporation and from 312 to 315 K for condensation. They found that the heat transfer enhancement ratio of the micro-fin tubes was 1.5 to 2 while the increase of press drop was only 40% when compared with smooth one at the same conditions. Chamra and Webb [3] investigated condensation heat transfer of R22 in 8 micro-fin tubes. The data were taken at the condensation temperature 297 K and the mass fluxes were from 41 to 181 kg m^{-2} s^{-1}. The cross grooved tubes had higher heat transfer coefficients than the single-helix ones with a maximum increase value of 27% at the same conditions. Li et al. [4] studied the condensation heat transfer coefficients of R22 in five micro-fin tubes with different geometries. The mass fluxes ranged from 200 to 650 kg m^{-2} s^{-1} and the saturation temperature was 320 K. The micro-fin tube with 50 fins had the largest enhancement ratio among the five tubes. The above studies mainly concentrated on the performance of different enhanced structures using R22 as working fluid. In the following presentation studies on condensation and boiling for R22 and its alternatives in micro-fin tubes will be briefly reviewed separately.

Miyara and Otsubo [5] performed an experiment to study the condensation heat transfer coefficients of R410A in three

* Corresponding author at: School of Energy and Power Engineering, Key Laboratory of Thermo-Fluid Science and Engineering of MOE, Xianning West Road, Xi'an, Shaanxi 710049, China. Tel./fax: +86 29 82669106.
E-mail address: wqtao@mail.xjtu.edu.cn (W.Q. Tao).

http://dx.doi.org/10.1016/j.ijheatmasstransfer.2016.03.024
0017-9310/

Nomenclature

A_o	the outside surface heat transfer area of tube [m^2]
A_i	the inside surface heat transfer area of tube [m^2]
c_p	the specific heat capacity of liquid [kJ kg^{-1} K^{-1}]
d_e	the equivalent diameter of casing channel [mm]
d_h	the fin height of micro-fin tube [mm]
d_i	the inside diameter of tube [mm]
d_o	the outside diameter of tube [mm]
h_i	in-tube heat transfer coefficients of tube [W m^{-2} K^{-1}]
h_l	the saturation liquid enthalpy of refrigerant [kJ kg^{-1}]
h_o	out-tube heat transfer coefficients of tube [W m^{-2} K^{-1}]
h_s	the latent heat of vaporization [kJ kg^{-1}]
h_v	the saturation vapor enthalpy of refrigerant [kJ kg^{-1}]
k	total heat transfer coefficients [W m^{-1} K^{-1}]
l	tube length [m]
M	molecular mass
m_w	the mass flux of water [kg s^{-1}]
n	the fin number
p_c	critical pressure [MPa]
Pr	Prandtl number
p_s	the refrigerant saturation pressure of test section [kPa]
q_w	the heat flux of test section in inner surface [W m^{-2}]
Δt_m	the logarithmic mean temperature difference of test section [°C]
Q_l	latent heat transfer capacity of the refrigerant [W]
Q_p	the heat transfer rate of preheater section [W]
Q_t	the heat transfer rate of test section [W]
t_i	the inlet water temperature inlet [°C]
t_o	the outlet water temperature inlet [°C]
t_{ri}	the inlet refrigerant temperature of test section [°C]
t_{ro}	the outlet refrigerant temperature of test section [°C]
t_s	the refrigerant saturation temperature of test section [°C]
$t_{water,i}$	the inlet water temperature of test section [°C]
$t_{water,o}$	the outlet water temperature of test section [°C]
t_{wi}	the average inner wall temperature of test section [°C]
t_{wo}	the average outer wall temperature of test section [°C]
x	the vapor quality of test section
x_i	the inlet vapor quality of test section
x_o	the outlet vapor quality of test section
α	the angle of fin [degree]
β	the helical angle of micro-fin tube [degree]
λ	thermal conductivity [W m^{-1} K^{-1}]
η_l	dynamic viscosity [Pa s]
σ	surface tension [mN m^{-1}]
ρ_l	the saturation liquid density of refrigerant [kg m^{-3}]
ρ_v	the saturation vapor density of refrigerant [kg m^{-3}]

herringbone micro-fin tubes with different fin height and helix angle. The mass fluxes ranged from 100 to 400 kg m^{-2} s^{-1} and the saturation temperature was 313 K. They found that the helical micro-fin tubes had lower heat transfer coefficients and higher pressure drop than those of herringbone tubes. Kim et al. [6] studied the condensation heat transfer of R22 and R410A in flat smooth/micro-fin aluminum multi-channel tubes. They found that the heat transfer coefficients of R410A was 5–10% larger than those of R22 for the smooth tube while 10–20% lower for the micro-fin tube. Jung et al. [7] conducted an experiment on condensation of R22, R134a, R407C, and R410A in 9.52 mm horizontal micro-fin/smooth tubes. The condensation temperature was 40 °C while the mass and heat fluxes were 100, 200, 300 kg m^{-2} s^{-1} and 7.7–7.9 kW m^{-2} respectively. They found that R134a and R410A had similar heart transfer performance to R22 while the heat transfer coefficients R407C were 11–15% lower than those of R22 for smooth tubes. For the micro-fin tube, R134a had similar heart transfer performance to R22 while R22 was better than R407C and R410A in their experimental results. Sapali and Patil [8] studied the condensation heat transfer of R134a and R404A in an 8.96 mm horizontal smooth/micro-fin tube. Their experimental results indicated that the condensation heat transfer coefficients decreased as condensing temperature increased for both smooth and micro-fin tubes. The heat transfer coefficients for R404A were 20–35% lower than those of R134a in their experiment. Zhang et al. [9] developed an experiment on condensation characters in 1.088 mm and 1.289 mm mini-tubes with R22, R410A and R407C as working fluids. They found that R410A had a better performance both in heat transfer and flow resistance compared with R22. Kondou and Hrnjak [10] investigated the condensation heat transfer of R744 and R410A in a 6.1 mm horizontal smooth tube. They found that the heat transfer coefficients of R744 were 20–70% higher than those of R410A at the same experimental conditions.

Kuo and Wang [11,12] investigated evaporation in a 9.52 mm horizontal micro-fin/smooth tube with R22 and R407C. The average heat transfer coefficients of the micro-fin tube were 2.2 times higher than those of the smooth one with R22 and the heat transfer coefficients and pressure drop of R407C was 50–80%, 30–50% respectively lower than those of R22 in their micro-fin tube. Lallemand et al. [13] obtained the boiling heat transfer coefficients in 12.7 mm horizontal smooth/micro-fin tubes with R22 and R407C. The refrigerant mass fluxes and heat fluxes were varied from 100 to 300 kg m^{-2} s^{-1} and 10 to 30 kW m^{-2}, respectively. Their experimental results showed that heat fluxes strongly influenced heat transfer at a low quality while the mass fluxes did that at a high quality and the boiling heat transfer coefficients of R407C in smooth and micro-fin tubes were 15–35% lower than those of R22. Greco and Vanoli [14] studied the heat transfer coefficients and pressure drop during the evaporation of R22 and R507 in a 6 mm horizontal smooth stainless steel tube. The heat transfer coefficients and pressure drop of R507 (R125–R143a 50%/50% in weight) were 10–30%, 30–50% respectively lower than those of R22 at the same conditions in their experiments. Kim and Shin [15] developed an experiment on evaporation of R22 and R410A in 9.52 mm horizontal smooth/micro-fin tubes. The evaporation heat transfer coefficients with R22 and R410A of the micro-fin tubes were 1.86–3.27, 1.64–2.99 times respectively larger than those of the smooth tube in their experiment. They found that the evaporating heat transfer coefficients of R410A were almost 12–29% larger than those of R22 at the same test conditions. Park and Hrnjak [16] obtained CO_2, R22 and R410A boiling flow characters in a 6.1 mm horizontal smooth tube. The evaporation temperatures, mass fluxes and heat fluxes were 15 and 30 °C, 100–400 kg m^{-2} s^{-1}, 5–15 kW m^{-2} respectively. The heat transfer coefficients for CO_2 were 2 times larger than those for R410A and R22 while the pressure drop of CO_2 was lower than that of R410A and R22 especially at low quality. Kundu et al. [17] investigated boiling in a 9.52 mm horizontal smooth tube of R134a and R407C. Their experimental results showed that the heat transfer coefficients and pressure drop of R134a were 55–87%, 53–86%

respectively higher than those of R407C at the same operating conditions.

As far as the heat transfer correlations are concerned, following studies are worth mentioning. Gungor and Winterton [18] developed a general correlation for flow boiling in vertical and smooth tubes after searching over 4300 data points for water, refrigerants and ethylene glycol from literature. The correlation could be used for saturated boiling in vertical and horizontal tubes, sub-cooled boiling and annuli. The mean deviation of the predicted heat transfer coefficients was 21.4% for saturated boiling and 25.0% for sub-cooled boiling compared with the based data. Yun et al. [19] proposed an evaporation correlation in horizontal micro-fin tubes of different refrigerants. A non-dimensional enhancement factor over smooth tubes correlation was used in their research and the correlation had a mean deviation of 20.5% compared with 749 data collected from the literature. Yoon et al. [20] studied the characteristics of evaporation heat transfer and pressure drop of carbon dioxide and developed a correlation of heat transfer coefficients. In their research, the test section was made of a 7.53 mm horizontal seamless smooth stainless steel tube with saturation temperature of −4 to 20 °C, mass fluxes of 200–530 kg m^{-2} s^{-1} and heat fluxes of 12–20 kW m^{-2}. They developed a new correlation by considering the critical quality (the quality at which liquid film breaks down) and the mean absolute deviation was 15.3%. Wang et al. [21] developed a theoretical model for water, R11 and ethylene glycol to predict film condensation heat transfer in square section horizontal micro-channels. Their model involved the influence of surface tension force, gravity, flow pattern, shear stress. The flow characters predicted by their model agreed well with physical phenomena which had an absolute average deviation of 15.3%. Cavallini et al. [22] presented a new model for predicting the condensation heat transfer coefficients in horizontal micro-fin tubes. The geometry enhancement factors predicted by their model agreed well with a mean absolute deviation of 16.5% compared with 3115 based data points among R22, R134a, R123, R410A and CO_2. Xu and Fang [23] obtained a new correlation of condensing pressure drop in different smooth pipes. They surveyed 525 experimental data points for 9 refrigerants in different micro tubes. Their correlation considering the Froude and Weber numbers had an absolute mean deviation 19.4% compared with based data points.

Although a great number of investigations on micro-fin tubes have been carried out, so far no any generally-accepted correlations for boiling heat transfer in different micro-fin tubes with different working medium exit in the literature. On the one hand this is due to micro-fin tubes differ from each other in several aspects, including tube inner diameter, fin number, fin cross-section geometry and the axial helical angle. Even for the single phase flow heat transfer in micro-fin tube great diversities of heat transfer correlations still exit [24,25]. On the other hand in-tube boiling heat transfer is a very complicated phenomenon. In order to develop a generally-accepted correlation much more reliable test data should be accumulated. This study investigates boiling heat transfer and pressure drop characteristics in a smooth and micro-fin tube which has been used in air-conditioning engineering in China. The working fluids include R22, R134a, R407C and R410A within a certain ranges of mass flux and heat flux. Apart from data accumulation, the other purpose of this paper is to search for the appropriate alternative of R22 from heat transfer point. The rest of the paper is organized as follows. In Section 2 the experimental system and the test ranges of several parameters will be presented. Data reduction method and uncertainty analysis will be discussed in Section 3. The test results will be provided in Section 4 with some discussions, including the thermo-hydraulic evaluation of the micro-fun tube compared with smooth tube. Finally some conclusions are drawn.

2. Experimental apparatus

Fig. 1 shows the schematic figure of the experimental apparatus. It consists of one refrigerant circulating system and four water circulating systems. Components of the refrigerant circulating system include a reservoir, a gear pump, a mass flow meter, a subcooler, a preheater, a test section and a condenser. The gear pump supplies refrigerant from the liquid reservoir to a mass flow meter. The refrigerant flow rate is measured by the mass flow meter with a nominal flow range of 0–136 kg h^{-1} and a relative accuracy of 0.10% in all scale. The mass flux of refrigerant in the experiment is controlled by adjusting the bypass pipe to the reservoir and the speed of gear pump motor managed by a variable-frequency drive. The refrigerant is sub-cooled in the subcooler and heated to a set-up quality in the preheater section at the entrance of the test section. In the test section, refrigerant is heated to a fixed quality. Finally, the two-phase refrigerant is condensed in the condenser and the sub-cooled liquid flows to the reservoir. The subcooler and condenser are two plate-fin heat exchangers with flowing cold water. It usually takes one hour to get the steady state. Components of the water circulating system include a thermostatic water bath, a centrifugal pump and an electromagnetic flowmeter. The water flow rate is measured by the electromagnetic flowmeter with a nominal flow range of 0–2.0 m^3 h^{-1} and a relative accuracy of 0.2% in all scale. The water flow rate is controlled by adjusting the bypass pipe to the bath and the speed of centrifugal pump motor which is controlled by a variable-frequency drive. The four water circulating systems provide water for the subcooler, preheater, test section and condenser in different heat flux.

The preheater section and test section are double-pipe heat exchangers with refrigerant in the inner side and water in the outer side. The outer pipe is a stainless steel pipe with inner diameter of 18.0 mm while the inner pipe is 1 m long smooth/micro-fin cooper tube with inner diameter of 8.76 mm and outside diameter of 9.52 mm. At the entrance and exit of test section, sheathed T-type thermocouples (1 mm outside diameter) with an uncertainty of ±0.1 °C are used to measure the temperature of refrigerant in the center of smooth/micro-fin cooper tube. The inlet and outlet pressure is measured by a pressure gage with a range of 0–2.5 MPa and a precision of ±6.25 kPa. A capacitive differential pressure sensor with a range of 0–37.4 kPa and a relative uncertainty of 0.2% in all scale is used to measure the pressure drop of test section. The schematic figure of the test section is shown in Fig. 2. The surface temperature of cooper tube is obtained by measuring the wall temperature in four equal interval cross sections at four periphery locations (the top, bottom, left and right direction) by copper-constantan thermocouples with a precision of ±0.2 °C. The thermocouples are welded with tin to ensure good contact with cooper tube wall. The outer wall temperature of cooper tube is assessed as the average of these sixteen thermocouples. Resistance temperature transducers (PT100) with a precision of ±0.15 °C are used to measure the temperature of the water flowing in and out the test section. The inlet temperature of water can be adjusted from 1 to 30 °C while the mass flow rate can be changed from 0.05 to 2.0 m^3 h^{-1}. The boiling heat flux can be adjusted in a range of 5–20 kW m^{-2}. The temperature of water bath is controlled by an independent refrigerant-cooled and electronically-heated system. The preheater section is similar to the test section without measuring the surface temperature and pressure drop. The T-type thermocouple electronic potential and temperature resistance are collected by a Keithley digital voltmeter.

The cross section geometries of the tested micro-fin tube are shown in Fig. 3 where two micro-photographs and a geometry diagram are displayed. Table 1 represents the geometrical

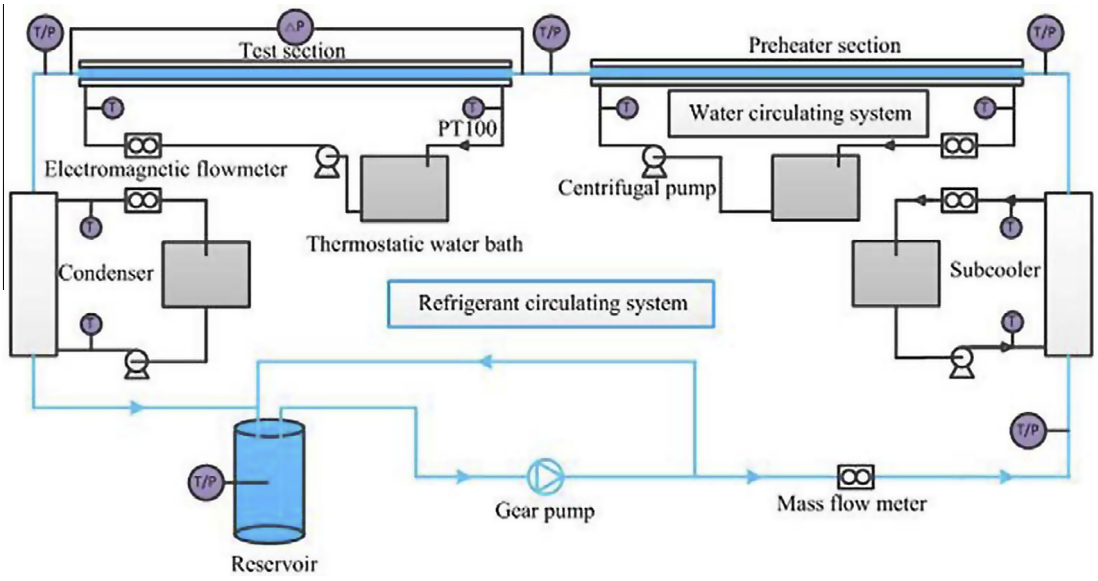

Fig. 1. Schematic diagram of the experimental apparatus.

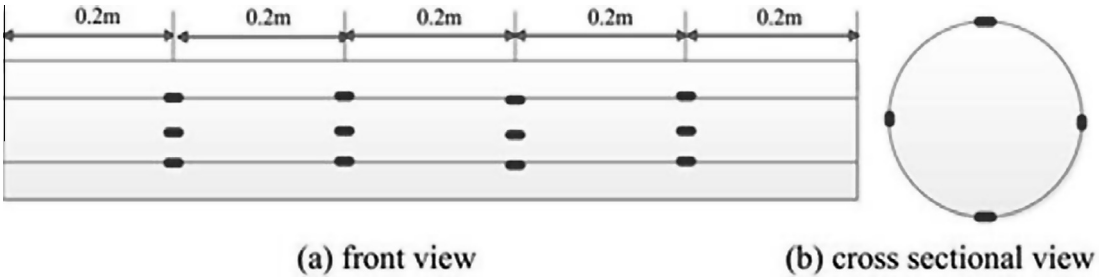

Fig. 2. The thermocouples arrangement diagram of the test section.

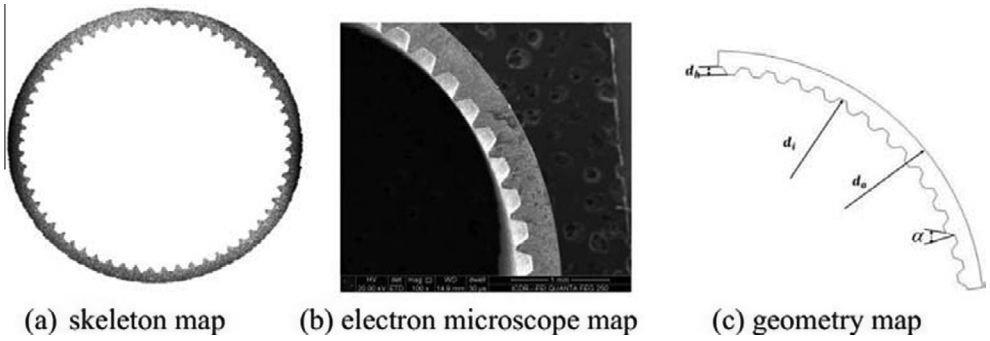

Fig. 3. Diagram of micro-fin tube.

Table 1
The geometrical parameters of the test tubes.

	d_o (mm)	d_i (mm)	n –	d_h (mm)	α (°)	β (°)
The smooth tube	9.52	8.76	–	–	–	–
The micro-fin tube	9.52	8.96	60	0.14	33	18

parameters of the test tubes. The inside surface area of micro-fin tube is 1.53 times larger than that of the smooth tube.

The experiment is conducted with R22, R134a, R407C and R410A at the boiling temperature of 5 °C. The mass fluxes and heat fluxes range from 50 to 450 kg m^{-2} s, and 5 to 20 kW m^{-2}, respectively. Refrigerant properties are obtained from NIST reference fluid property and are summarized in Table 2.

3. Data reduction and uncertainty analysis

The in-tube boiling heat transfer coefficients of cooper tube are determined by the following equation:

$$h_i = \frac{q_w}{t_{wi} - t_s} \tag{1}$$

where q_w is the heat flux at the test section while t_{wi} and t_s is the temperature of inside wall and the saturation temperature of refrigerant.

Table 2
Fluid properties of refrigerant in test conditions.

	t_s (°C)	p_s (kPa)	ρ_l (kg/m^3)	h_l (kJ/kg)	h_v (kJ/kg)	h_s (kJ/kg)	λ_l (mW/m K)	η_l (μPa s)	p_c (MPa)	σ (mN/m)	M –	Pr_l –
R22	5	584.1	1264.3	205.9	406.9	201	92.5	204.5	4.75	10.95	86.48	2.62
R134a	5	349.7	1278.1	206.8	401.5	194.7	89.8	250.1	4.07	10.84	102.03	3.77
R407C	5	666	1217.7	207.1	411.8	204.7	93.8	198	4.62	10.29	86.2	3.03
R410A	5	936.2	1149.6	207.7	422.7	215	100.2	191.9	4.95	8.38	72.58	2.34

The inner wall heat flux and average temperature is determined by Eqs. (2) and (3), respectively:

$$q_w = \frac{c_p m_w (t_i - t_o)}{A_i} \tag{2}$$

$$t_{wi} = t_{wo} - \frac{q_w d_i^2}{8\lambda} \ln \frac{d_o}{d_i} \tag{3}$$

where t_i and t_o stands for the inlet and outlet water temperature and

$$t_{wo} = \frac{\sum_{i=1}^{16} t_{wo_i}}{16} \tag{4}$$

It should be noted here that for the micro-fin tube the inner surface area is determined by its embryo tube with an inner diameter of 8.68 mm in the experiment.

The vapor quality of test section at the inlet and outlet is calculated from energy conservation of the preheater section and test section. The mean vapor quality of the test section is defined by Eq. (5):

$$x = \frac{x_i + x_o}{2} \tag{5}$$

$$x_i = \frac{Q_p - Q_l}{m_r q_s} \tag{6}$$

$$x_o = \frac{Q_t}{m_r q_s} + x_i \tag{7}$$

where Q_p and Q_t is the heat transfer rate of preheater and test section while Q_l is the explicit heat transfer rate of the refrigerant for heating it up to the saturated temperature in the preheater section.

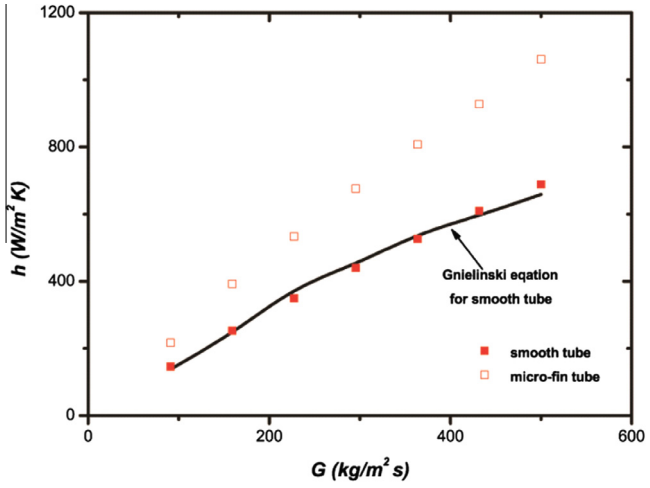

Fig. 4. The single phase heat transfer coefficients of the smooth and micro-fin tube with R22.

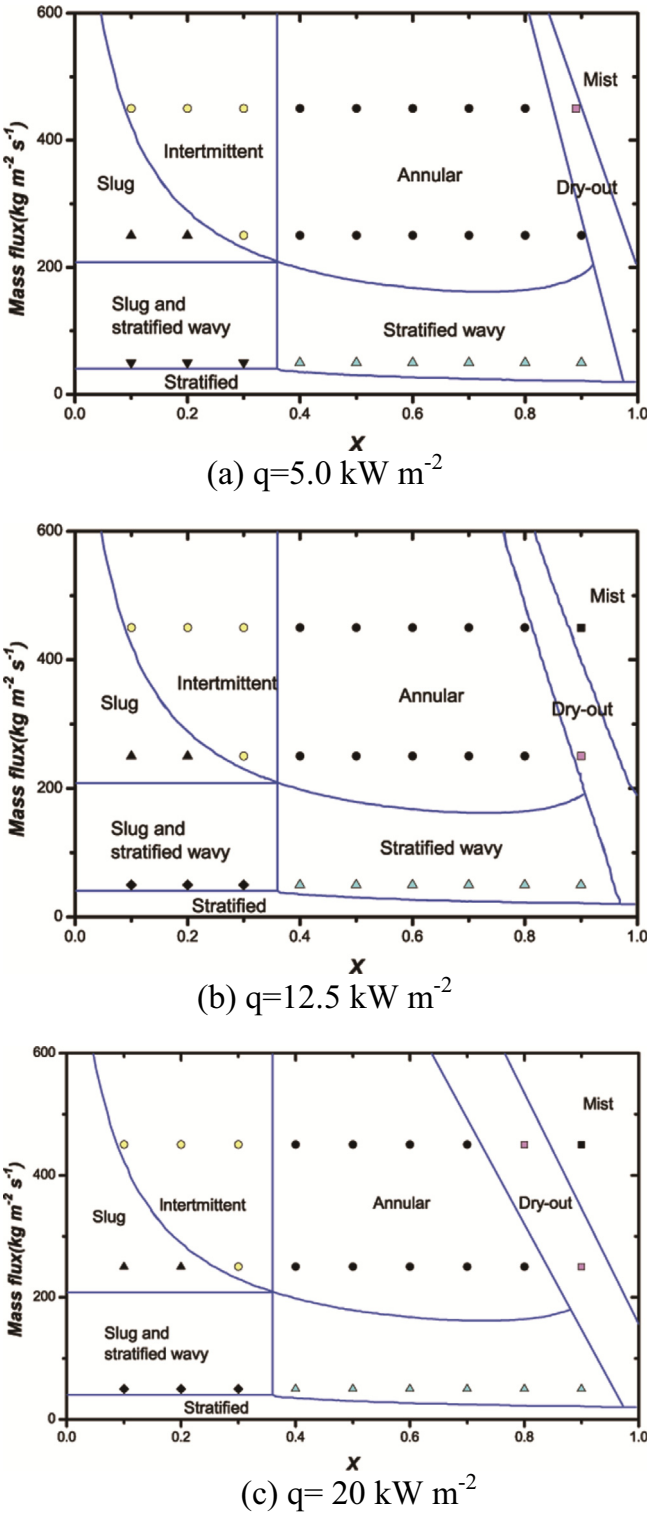

Fig. 5. Flow patterns of the test data on the map of Wojtan et al. [27] for R22 in the smooth tube.

Uncertainty analysis is performed according to Ref. [26]. Based on the equations above and the precision of experimental instruments, the maximum estimated relative uncertainty of in-tube single phase and boiling heat transfer coefficients of smooth/micro-fin tubes is 7.2% and 9.1%, respectively.

4. Results and discussions

4.1. Single phase heat transfer results

The energy unbalance is researched in single phase flow before conducting the boiling heat transfer. The difference between refrigerant and water side heat flux is always within ±5% deviation which certifies the energy conservation in our experiment. Well heat preservation is done to prevent heat loss and the heat leakage can be controlled within 5%. Fig. 4 shows the single phase heat transfer characters of smooth and micro-fin tubes. The black line represents calculated results of smooth tube by Gnielinski Equation. Our results are reliable because the experimental data of the smooth tube are within ±8% deviation compared with the predicted data. The heat transfer coefficients of micro-fin tubes are higher than those of smooth tube, which can be explained by

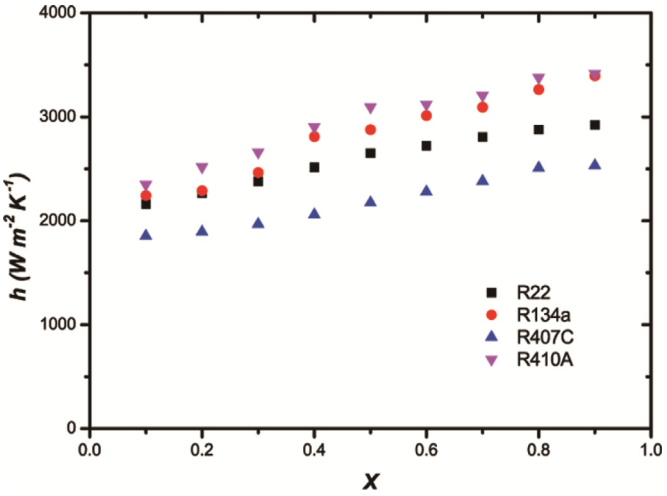

(a) G=50 kg m^{-2} s^{-1}

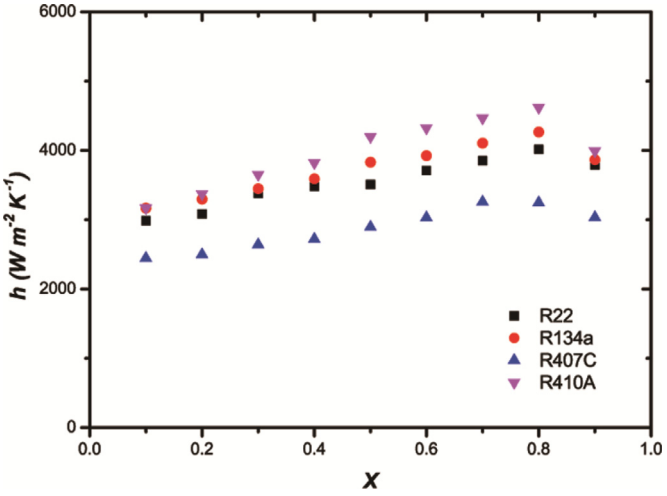

(b) G=250 kg m^{-2} s^{-1}

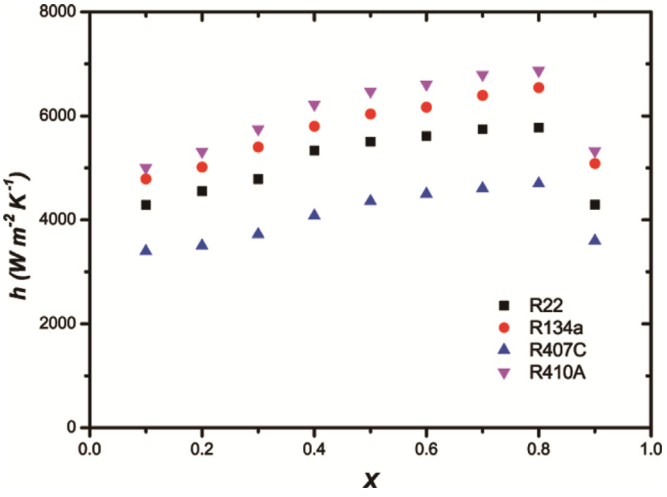

(c) G=450 kg m^{-2} s^{-1}

Fig. 6. The heat transfer coefficients of the smooth tube with different refrigerant (q = 12.5 kW m^{-2}).

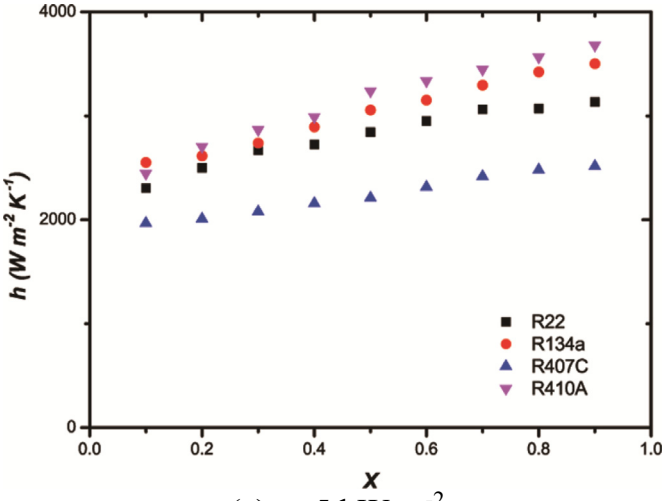

(a) q=5 kW m^{-2}

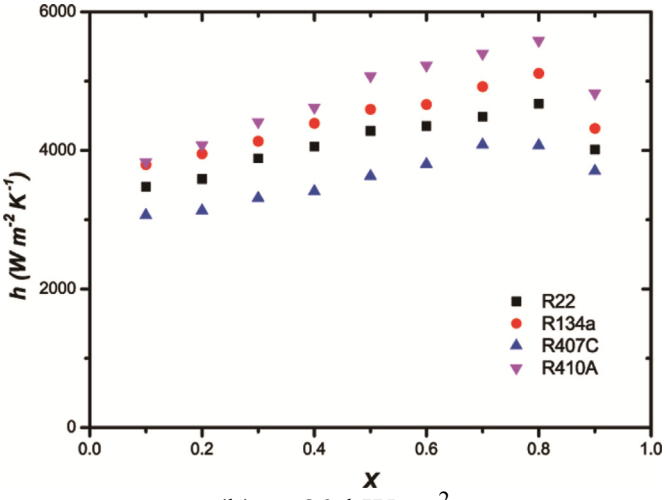

(b) q=20 kW m^{-2}

Fig. 7. The heat transfer coefficients of the smooth tube with different refrigerant (G = 250 kg m^{-2}).

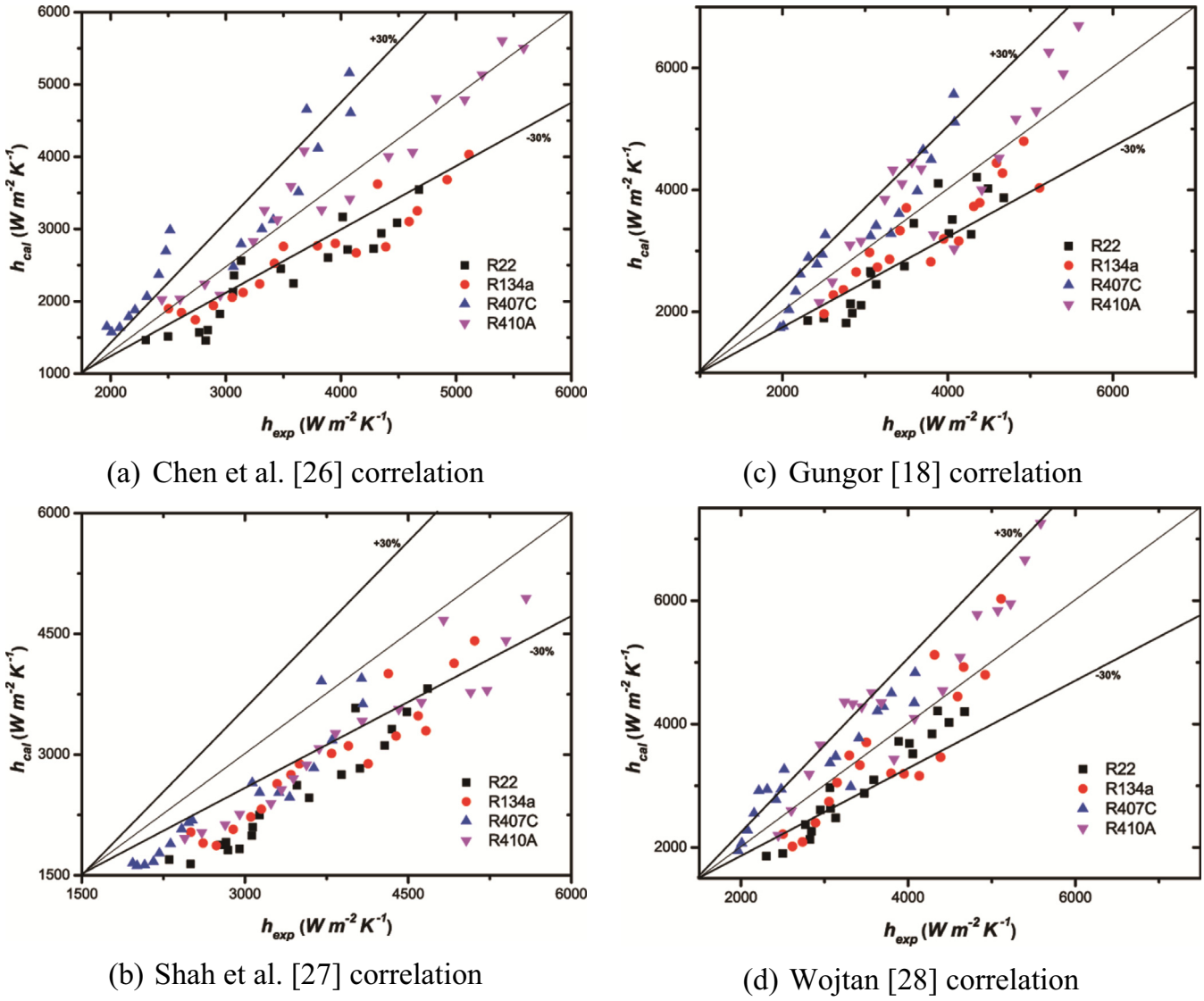

Fig. 8. Comparison of experimental results with four heat transfer correlations.

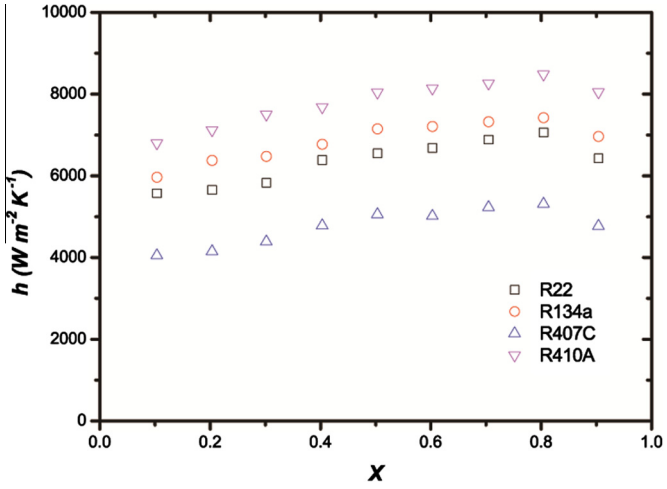

Fig. 9. The HTCs of the micro-fin tube with different refrigerant (G = 250 kg m^{-2}, q = 12.5 kW m^{-2}).

the flow disturbance and larger heat transfer area caused by micro-fin.

4.2. Flow pattern identification for smooth tube test data

It is impossible to observe the flow pattern when studying heat transfer and pressure drop characters in a metal tube. Here we use the map of Wojtan et al. [27]. All the test results of R22 for smooth tube are presented on this flow pattern map in Fig. 5 to identify the flow patterns of the test data, where the vapor quality shown in the abscissa is the averaged vapor quality in the entire test section. This flow pattern map is constructed without heat transfer in a transparent pipe and widely accepted in literatures. The data are measured at t_s = 5 °C and mass flux = 50, 250, 450 kg m^{-2} s^{-1} while heat flux = 5, 12.5, 20 kW m^{-2}. By adjusting the inlet vapor quality of the test section, almost the same average vapour quality at different heat flux can be obtained. It can be seen from the figure that at lower mass flux G = 50 kg m^{-2} s^{-1}, the flow regimes of the test data are stratified wavy with slug at low vapor quality in different heat flux. For mass flux G = 250 kg m^{-2} s^{-1}, slug, intermittent and annular flow pattern is observed with the increase of vapor quality, then dry-out occurs at high vapor quality. At G = 450 kg m^{-2} s^{-1},

intermittent, annular flow is respectively achieved with the increase of vapor quality and finally dry-out and mist regimes occur at high vapor quality. It can be observed that the data distribute in the flow pattern maps uniformly. Some minor differences occur at middle and high mass flow rate with some data being in the dry-out and mist regimes.

4.3. Boiling heat transfer results

4.3.1. Comparison of smooth tube results with existing correlations

Fig. 6 presents the smooth tube heat transfer coefficients of R22, R134a, R407C and R410A at t_s = 5 °C, mass flux = 50, 250, 450 kg m^{-2} s^{-1} and heat flux = 12.5 kW m^{-2}. The vapor quality is the average value of inlet and outlet in the test section. The heat transfer coefficients are the mean HTCs for the test section. Three meaningful features can be observed in the figure. First for the three mass flow rates studied at the same vapor quality and heat flux, the heat transfer coefficients of 410a are the highest while those of 407C are the lowest. For the case of mass flow rate = 50 kg m^{-2} s^{-1}, the HTCs of R410A are 12% higher than those of R22, and the HTCs of R134a are about 10% higher in large vapor quality region. For mass flow rate = 250 and 450 kg m^{-2} s^{-1}, the HTCs of R410A and R134a are 14–25% and 8–15% higher than those of R22, respectively. The HTCs of R407C are 18–32% lower than R22's for all test mass flux. Second, the HTCs of all refrigerants increase with the mass flux in the entire vapor quality region. Third, the vapor quality has a positive effect on the HTCs until the flow goes into the dry-out and mist flow regimes, where a sharp decrease in HTC with vapor quality occurs.

The HTCs of the four refrigerants under different heat flux (q = 5, 20 kW m^{-2}) at t_s = 5 °C and G = 250 kg m^{-2} s^{-1} are shown in Fig. 7. The same features indicated in the above paragraph can be observed. The average heat transfer coefficients of R410A, R134a and R407C are 125.2%, 110.9% and 78.0% of those of R22, respectively.

The comparisons of our experimental results in this study with correlations of Chen et al. [28], Shah et al. [29], Gungor et al. [18] and Wojtan et al. [30] are shown in Fig. 8(a)–(d) respectively. It can be seen that for these 72 test data of four refrigerants, the correlations of Gungor et al. [18] and Wojtan et al. [30] have the best agreement, with deviations of 54 and 50 data being within ±30%, respectively. The maximum deviations of the two correlations are 45% and 39%, respectively. The agreement with the correlation of Chen et al. [28] ranks second, where 38 data points are predicted within ±30% deviation, and the maximum deviation is 53%. There is a systematic negative deviation between the data in this study and the correlation of Shah et al. [29]. Among 72 data in this study, 71 are under-predicted, and the averaged deviation is −32%.

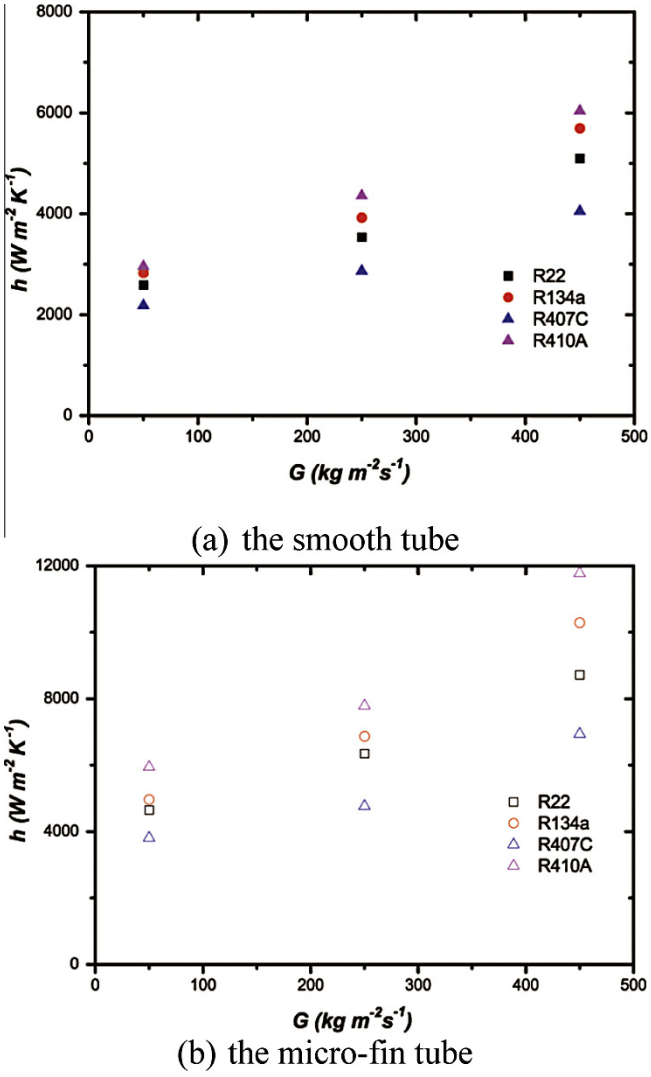

Fig. 10. Effect of mass flux on the HTCs with different refrigerant (q = 12.5 kW m^{-2}).

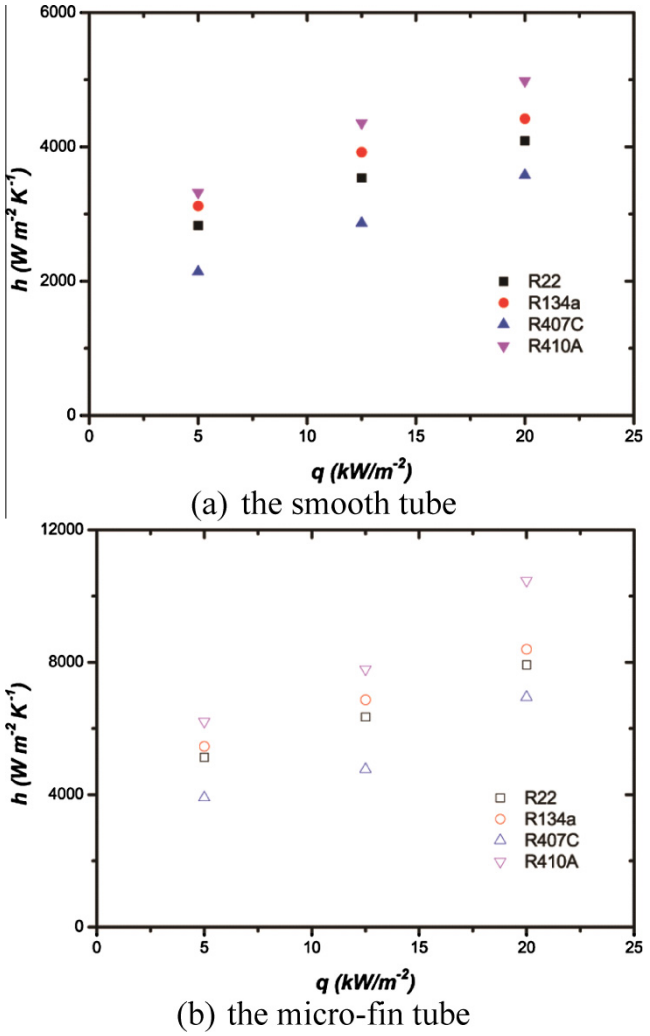

Fig. 11. Effect of heat flux on the HTCs with different refrigerant (G = 250 kg m^{-2}).

4.3.2. Results of micro-fin tubes

The heat transfer coefficients of R22, R134a, R407C and R410A for the micro-fin tube tested at saturation temperature 5 °C with a mass flux of 250 kg m^{-2} s^{-1} and heat flux of 12.5 kW m^{-2} are shown in Fig. 9, where the corresponding data of smooth tube are also presented for comparison. It can be observed that the variation patterns of the HTCs of all refrigerants in the micro-fin tube with vapor quality are quite similar to those of the smooth tube. The micro-fin tube can enhance boiling heat transfer significantly. The ratio of the HTCs for the micro-fin tube over those of smooth tube with 22, R134a, R407C and R410A is 1.80, 1.84, 1.56 and 1.75 respectively.

Figs. 10 and 11 present the variation of the mean HTCs with the mass flow rate and heat flux, respectively. As shown in the figures, the mean HTCs increase as the mass flow rate and heat flux increases for both the smooth and micro-fin tube. For a comprehensive estimation and comparison, the average heat transfer coefficients for four refrigerants in all test conditions (G = 50, 250 and 450 kg m^{-2} s^{-1} while q = 5, 12.5 and 20 kW m^{-2}) for the smooth and micro-fin tube are shown in Table 3. The average heat transfer coefficients of R22, R134a, R407C and R410A are 1.86, 1.80, 1.69 and 1.78 times higher than those of the smooth tube.

An attempt is made to compare our test data with the existing correlations for the micro-fin tube reported in [19,31] and as large as 80% deviations is found. The comparison with correlation of [31] is shown in Fig. 12. Since test data for smooth tubes in the study agree well with most existing correlations as shown above, it is our consideration that the large deviation is caused by the imperfectness of the existing correlations for the micro-fin tubes. No attempt is made to correlate our own data because they are obtained only for one micro-fin tube. As indicated above, it is the authors' suggestion that our international heat transfer community should accumulate much more data for different types of micro-fin tubes and for different refrigerants. Test data in this study for the micro-fin tube are shown in the supporting information, which is expected to make a contribution to the establishment of a generally-accepted correlation.

Table 3
The average HTCs with four refrigerants in all test conditions.

	R22	R134a	R407C	R410A
The smooth tube (kW m^{-2} K^{-1})	3.74	4.08	3.03	4.32
The micro-fin tube (kW m^{-2} K^{-1})	6.96	7.34	5.13	7.69
Increase ratio	1.86	1.80	1.69	1.78

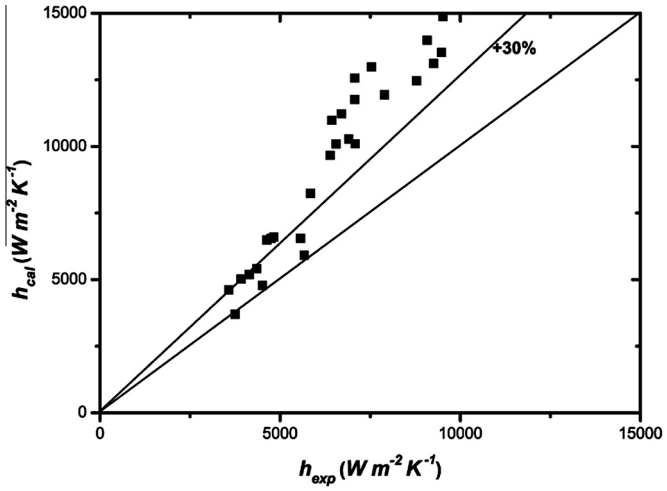

Fig. 12. Comparison of micro-fin tube experimental results with Chiou [31] correlation.

4.4. Pressure drop results

Fig. 13 presents the pressure gradient of four refrigerants for the smooth and micro-fin tube at a mass flux of 250 kg m^{-2} s^{-1} and a heat flux of 12.5 kW m^{-2}. The vapor quality is the average value of the inlet and outlet in the test section. The pressure gradient is the mean value of the test section. As the vapor quality increases, the pressure drop of all fluids increases almost linearly. The pressure drop of R22, R407C and R410A is quite close to each other in both the smooth and micro-fin tube while the pressure drop of R134a is 1.7 times higher than that of the smooth tube and 1.55 times higher than the micro-fin tube of R22. As shown in Table 2, this difference is mainly caused by their different dynamic viscosity.

The average pressure drop for four refrigerants in all test conditions (G = 50, 250 and 450 kg m^{-2} s^{-1} while q = 5, 12.5 and 20 kW m^{-2}) for the smooth and micro-fin tube is shown in Table 4. The average pressure drop of R22, R134a, R407C and R410A is 1.42, 1.30, 1.45 and 1.40 times higher than that of the smooth tube.

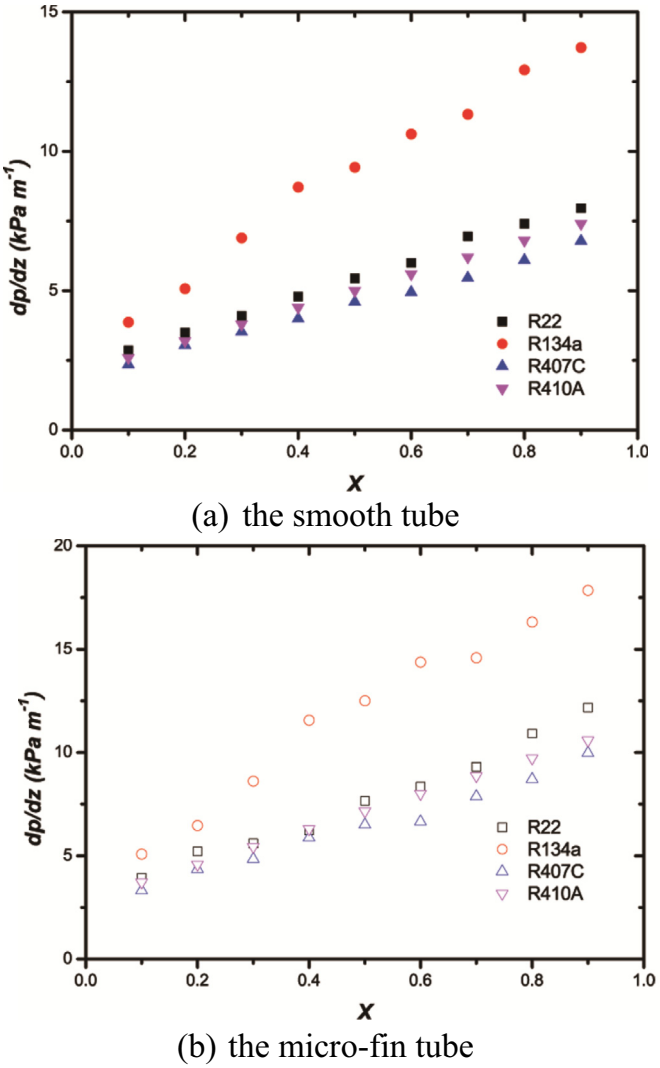

Fig. 13. The pressure drop with different refrigerant (G = 250 kg m^{-2}, q = 12.5 kW m^{-2}).

Table 4
The average pressure drop for four refrigerants in all test conditions.

	R22	R134a	R407C	R410A
The smooth tube (kPa)	5.45	9.17	4.54	5.09
The micro-fin tube (kPa)	7.71	11.92	6.56	7.15
Increase ratio	1.42	1.30	1.45	1.40

4.5. Efficiency index

It is a well-known fact that heat transfer enhancement must be followed by a penalty of pressure drop increase. Thus to evaluate an enhanced structure more reasonably, its thermohydraulic performance should be considered. For both single-phase and multiphase flow and heat transfer, different criteria have been proposed [32,33]. For phase change heat transfer, Chamra et al. [33] proposed following criteria, called efficiency index η_1, to evaluate the performance of micro-fin tubes defined as follows:

$$\eta_1 = \frac{h_m/h_s}{\Delta p_m/\Delta p_s} \tag{8}$$

where h_s and h_m is the HTCs of the smooth and micro-fin tube while Δp_s and Δp_m is the pressure drop of the smooth and micro-fin tube respectively. The numerator of Eq. (8) is the average heat transfer coefficients increase ratio as shown in Table 3 and the denominator is the average pressure drop increase ratio as shown in Table 4. This efficiency index η_1 of the micro-fin tube for R134a, R22, R410A, and R407C is 1.38, 1.31, 1.27 and 1.17 respectively.

The ratio η_1 means that the performance of the micro-fin tube is evaluated at the same flow rate. Sometimes the evaluation may be conducted under the constraints of identical pressure drop or identical pumping power of driving the refrigerant [32], and here we denote them by η_2, η_3, respectively:

$$\eta_2 = \frac{h_m/h_s}{(\Delta p_m/\Delta p_s)^{1/2}} \tag{9}$$

$$\eta_3 = \frac{h_m/h_s}{(\Delta p_m/\Delta p_s)^{1/3}} \tag{10}$$

Based on the previous data, for R134a, R22, R410A, and R407C the values of η_2 are 1.58, 1.56, 1.50 and 1.40 respectively, those of η_3 are 1.66, 1.65, 1.59 and 1.49 respectively.

5. Conclusions

An experimental study of R22, R134a, R407C and R410A boiling heat transfer in 9.52 mm smooth and micro-fin tube has been investigated at saturation temperature of 5 °C with mass flux 50, 250, 450 kg m^{-2} s^{-1} and heat flux of 5, 12.5, 20 kW m^{-2}. The heat transfer and pressure drop performances for four refrigerants in different condition are obtained and the following conclusions can be drawn:

(1) For the smooth tube, the average heat transfer coefficients of R134a, R407C and R410A are 110.9%, 78.0% and 125.2% of those of R22 in test conditions and the heat transfer results agree well when compared with Gungor et al. [18] correlation and Wojtan et al. [30] correlation.
(2) For the micro-fin tube, the average heat transfer coefficients of R22, R134a, R407C and R410A are 1.86, 1.80, 1.69 and 1.78 times higher than those of the smooth tube. The micro-fin tube enhances heat transfer greatly.
(3) For the smooth tube, the pressure drop of R22, R407C and R410A is close to each other while the pressure drop of R134a is 1.7 times higher. For the micro-fin tube, the average pressure drop of R22, R134a, R407C and R410A are 1.42, 1.30, 1.45 and 1.40 times higher than that of the smooth one.
(4) The thermo-hydraulic performance of the micro-fin tube may be evaluated by the efficiency index η_1, η_2, η_3 respectively at the identical flow rate, identical pressure drop and identical power consumption. For the tested micro-fin tube, the values of η_1 for R22, R134a, R407C and R410A are 1.31, 1.38, 1.17 and 1.27 respectively. The values of η_2 are 1.56, 1.58, 1.40 and 1.50 respectively while those of η_3 are 1.65, 1.66, 1.49 and 1.59, respectively.

Acknowledgments

This study was supported by the National Key Basic Research Program of China (973 Program) (2013CB228304) and the 12th Five-Year National Key Technology R & D Program (2012BAA10B01).

Appendix A

Appendix experimental data for micro-fin tube.

Vapor quality	Heat flux (kW m^{-2})	Mass flux (kg m^{-2} s^{-1})	h_i (W m^{-2} K^{-1})			
			R22	R134a	R407C	R410A
0.1	5	50	2872.0	2867.4	2406.6	3279.1
0.2	5	50	3012.0	2926.1	2459.0	3515.7
0.3	5	50	3161.3	3150.1	2556.6	3713.7
0.4	5	50	3341.2	3592.8	2673.2	4053.9
0.5	5	50	3521.8	3677.7	2825.8	4220.3
0.6	5	50	3616.8	3849.8	2961.3	4356.1
0.7	5	50	3727.8	3953.1	3094.1	4473.9
0.8	5	50	3823.5	4171.8	3260.0	4715.6
0.9	5	50	3883.4	4340.4	3289.4	4766.2
0.1	5	250	3986.7	4351.9	3041.8	4554.7
0.2	5	250	4322.2	4548.8	3105.7	4846.4
0.3	5	250	4790.4	4761.2	3212.7	5244.9

Appendix A (*continued*)

Vapor quality	Heat flux (kW m^{-2})	Mass flux (kg m^{-2} s^{-1})	h_i (W m^{-2} K^{-1})			
			R22	R134a	R407C	R410A
0.4	5	250	4886.5	5031.6	3336.3	5493.1
0.5	5	250	4919.1	5314.0	3420.3	6031.1
0.6	5	250	5102.1	5480.5	3579.0	6211.6
0.7	5	250	5298.2	5732.5	3737.5	6417.0
0.8	5	250	5313.3	5954.8	3835.0	6638.7
0.9	5	250	5419.5	6090.0	3890.7	6853.2
0.1	5	450	5697.8	6118.0	4408.9	6982.6
0.2	5	450	6051.1	6411.0	4551.2	7420.7
0.3	5	450	6360.1	6906.4	4833.1	8020.8
0.4	5	450	7085.2	7415.4	5300.5	8681.9
0.5	5	450	7315.6	7717.6	5661.6	9033.6
0.6	5	450	7459.2	7886.1	5841.4	9225.0
0.7	5	450	7629.4	8173.3	5982.7	9479.7
0.8	5	450	7807.9	8363.3	6101.7	9592.6
0.9	5	450	8096.4	8543.9	6229.9	9667.2
0.1	12.5	50	3575.6	3609.5	2834.6	4063.6
0.2	12.5	50	3749.5	3663.4	2896.3	4356.9
0.3	12.5	50	3914.9	3965.3	3011.2	4602.3
0.4	12.5	50	4138.2	4522.6	3168.6	5123.8
0.5	12.5	50	4352.5	4629.5	3328.3	5354.0
0.6	12.5	50	4510.3	4846.1	3487.9	5398.3
0.7	12.5	50	4628.2	4996.1	3624.3	5644.3
0.8	12.5	50	4747.0	5251.4	3839.7	5843.8
0.9	12.5	50	4821.4	5463.7	3874.4	5906.5
0.1	12.5	250	5565.3	5955.5	4053.0	6835.0
0.2	12.5	250	5666.2	6379.8	4162.3	7117.4
0.3	12.5	250	5842.5	6493.9	4400.6	7492.9
0.4	12.5	250	6391.6	6787.7	4791.4	7684.2
0.5	12.5	250	6550.3	7180.8	5068.8	8053.3
0.6	12.5	250	6705.7	7209.4	5038.6	8161.6
0.7	12.5	250	6905.9	7347.8	5238.6	8250.0
0.8	12.5	250	7073.3	7425.0	5346.0	8478.2
0.9	12.5	250	6436.5	6989.5	4790.1	8064.9
0.1	12.5	450	7074.0	7701.3	5193.0	8653.2
0.2	12.5	450	7532.6	8070.1	5360.5	9096.1
0.3	12.5	450	7896.2	8673.8	5662.6	9939.8
0.4	12.5	450	8786.5	9334.5	6243.1	10759.1
0.5	12.5	450	9082.6	9714.9	6668.4	11095.0
0.6	12.5	450	9260.9	9927.0	6880.1	11432.1
0.7	12.5	450	9482.1	10298.6	7076.6	11747.8
0.8	12.5	450	9518.7	10527.7	7186.8	11887.6
0.9	12.5	450	7082.0	8189.1	5501.8	9212.1
0.1	20	50	4813.0	5268.6	4587.8	6717.8
0.2	20	50	5050.5	5682.2	4548.9	6595.0
0.3	20	50	5299.5	5752.1	4899.1	7244.6
0.4	20	50	5823.7	6117.9	5331.4	7729.4
0.5	20	50	6126.6	6389.2	5658.0	8211.1
0.6	20	50	6062.9	6540.8	5767.2	8619.8
0.7	20	50	6249.1	6421.4	5664.2	8294.1
0.8	20	50	6186.6	6231.9	5366.6	8091.7
0.9	20	50	5767.3	5984.9	5140.0	7787.2
0.1	20	250	6014.2	6604.7	4740.2	7135.3
0.2	20	250	6207.4	6872.9	4845.1	7592.3
0.3	20	250	6723.1	7190.0	5122.2	8216.6
0.4	20	250	7017.8	7636.2	5274.4	8605.3
0.5	20	250	7410.7	7989.9	5615.4	9448.2
0.6	20	250	7526.7	8113.5	5875.9	9730.9
0.7	20	250	8092.4	8895.1	6296.3	10400.0
0.8	20	250	7762.8	8563.0	6313.9	10052.7

(*continued on next page*)

Appendix A (*continued*)

Vapor quality	Heat flux (kW m^{-2})	Mass flux (kg m^{-2} s^{-1})	h_i (W m^{-2} K^{-1})			
			R22	R134a	R407C	R410A
0.9	20	250	6946.5	7511.0	5725.5	8985.8
0.1	20	450	9774.2	10356.8	8840.8	13309.3
0.2	20	450	10367.8	10508.8	8763.4	13583.9
0.3	20	450	10553.2	10752.1	9258.2	13969.6
0.4	20	450	10899.7	11353.6	9876.7	14219.3
0.5	20	450	11217.5	11861.3	10417.0	14975.8
0.6	20	450	11712.6	12164.0	11305.7	16332.0
0.7	20	450	11485.1	11902.9	10808.1	15700.7
0.8	20	450	11368.0	12261.8	11172.2	15845.3
0.9	20	450	11385.0	11610.3	10273.0	15221.9

References

[1] K. Fujie, M. Itoh, T. Innami, H. Kimura, W. Nakyama, T. Yanagida, Heat transfer pipe, US patent 4,044,797, 1977 [assigned to Hitachi, Ltd.].
[2] L.M. Schlager, M.B. Pate, A.E. Bergles, Evaporation and condensation heat transfer and pressure drop in horizontal 12.7 mm microfin tubes with refrigerant 22, J. Heat Transfer 112 (1990) 1041–1047.
[3] M.L. Chamra, R.L. Webb, M.R. Randlett, Advanced micro-fin tubes for condensation, Int. J. Heat Mass Transfer 39 (1996) 1839–1846.
[4] G.Q. Li, Z. Wu, W. Li, Z.K. Wang, X. Wang, H.X. Li, S.C. Yao, Experimental investigation of condensation in micro-fin tubes of different geometries, Exp. Thermal Fluid Sci. 37 (2012) 19–28.
[5] A. Miyara, Y. Otsubo, Condensation heat transfer of herringbone micro fin tubes, Int. J. Therm. Sci. 41 (2002) 639–645.
[6] N.H. Kim, J.P. Cho, J.O. Kim, B. Youn, Condensation heat transfer of R-22 and R-410A in flat aluminum multi-channel tubes with or without micro-fins, Int. J. Refrig. 26 (2003) 830–839.
[7] D. Jung, Y. Cho, K. Park, Flow condensation heat transfer coefficients of R22, R134a, R407C, and R410A inside plain and micro-fin tubes, Int. J. Refrig. 27 (2004) 25–32.
[8] S.N. Sapali, P.A. Patil, Heat transfer during condensation of HFC-134a and R-404A inside of a horizontal smooth and micro-fin tube, Exp. Thermal Fluid Sci. 34 (2010) 1133–1141.
[9] H.Y. Zhang, J.M. Li, N. Liu, B.X. Wang, Experimental investigation of condensation heat transfer and pressure drop of R22, R410A and R407C in mini-tubes, Int. J. Heat Mass Transfer 55 (2012) 3522–3532.
[10] C. Kondou, P. Hrnjak, Condensation from superheated vapor flow of R744 and R410A at subcritical pressures in a horizontal smooth tube, Int. J. Heat Mass Transfer 55 (2012) 2779–2791.
[11] C.S. Kuo, C.C. Wang, In-tube evaporation of HCFC-22 in a 9.52 mm micro-fin/smooth tube, Int. J. Heat Mass Transfer 39 (1996) 2556–2569.
[12] C.S. Kuo, C.C. Wang, Horizontal flow boiling of R22 and R407C in a 9.52 mm micro-fin/smooth tube, Appl. Therm. Eng. 16 (1996) 713–731.
[13] M. Lallemand, C. Branescu, P. Haberschill, Local heat transfer coefficients during boiling of R22 and R407C in horizontal smooth and micro-fin tubes, Int. J. Refrig. 24 (2001) 57–72.
[14] A. Greco, G.P. Vanoli, Evaporation of refrigerants in a smooth horizontal tube: prediction of R22 and R507 heat transfer coefficients, Appl. Therm. Eng. 24 (2004) 2189–2206.
[15] M.H. Kim, J.S. Shin, Evaporating heat transfer of R22 and R410A in horizontal smooth and micro-fin tubes, Int. J. Refrig. 28 (2005) 940–948.
[16] C.Y. Park, P.S. Hrnjak, CO_2 and R410A flow boiling heat transfer, pressure drop, and flow pattern at low temperatures in a horizontal smooth tube, Int. J. Refrig. 30 (2007) 166–178.
[17] A. Kundu, R. Kumar, A. Gupta, Heat transfer characteristics and flow pattern during two-phase flow boiling of R134a and R407C in a horizontal smooth tube, Exp. Thermal Fluid Sci. 57 (2014) 344–352.
[18] K.E. Gungor, R.H.S. Winterton, A general correlation for flow boiling in tubes and annuli, Int. J. Heat Mass Transfer 29 (1986) 351–358.
[19] W.W. Wang, T.D. Radcliff, R.N. Christensen, A condensation heat transfer correlation for millimeter-scale tubing with flow regime transition, Exp. Thermal Fluid Sci. 26 (2002) 473–485.
[20] S.H. Yoon, E.S. Cho, Y.W. Hwang, M.S. Kim, K. Kim, Y. Kim, Characteristics of evaporative heat transfer and pressure drop of carbon dioxide and correlation development, Int. J. Refrig. 27 (2004) 111–119.
[21] H.S. Wang, J.W. Rose, H. Honda, A theoretical model of film condensation in square section horizontal microchannels, Chem. Eng. Res. Des. 82 (2004) 430–434.
[22] A. Cavallini, D.D. Col, S. Mancin, L. Rossetto, Condensation of pure and near-azeotropic refrigerants in microfin tubes: a new computational procedure, Int. J. Refrig. 32 (2009) 162–174.
[23] Y. Xu, X. Fang, A new correlation of two-phase frictional pressure drop for condensing flow in pipes, Nucl. Eng. Des. 263 (2013) 87–96.
[24] W.T. Ji, D.C. Zhang, Y.L. He, W.Q. Tao, Prediction of fully developed turbulent heat transfer of internal helically ribbed tubes – An extension of Gnielinski equation, Int. J. Heat Mass Transfer 55 (2012) 1375–1384.
[25] W.T. Ji, A.M. Jacobi, Y.L. He, W.Q. Tao, Summary and evaluation on single-phase heat transfer enhancement techniques of liquid laminar and turbulent pipe flow, Int. J. Heat Mass Transfer 88 (2015) 735–754.
[26] S.J. Kline, F.A. Mcclintock, Describing uncertainties in single-sample experiments, Mech. Eng. 75 (1953) 3–8.
[27] L. Wojtan, T. Ursenbacher, J.R. Thome, Investigation of flow boiling in horizontal tubes: Part I – A new diabatic two phase flow pattern map, Int. J. Heat Mass Transfer 48 (2005) 2955–2969.
[28] J.C. Chen, Correlation for boiling heat-transfer to saturated fluids in convective flow, Ind. Eng. Chem. Process Des. Dev. 5 (3) (1966) 322–339.
[29] M.M. Shah, Chart characteristics for saturated boiling heat transfer: equation and further study, ASHRAE Transfer 88 (1) (1982) 185–196.
[30] L. Wojtan, T. Ursenbacher, J.R. Thome, Investigation of flow boiling in horizontal tubes. Part II: Development of a new heat transfer model for stratified-wavy, dry-out and mist flow regimes, Int. J. Heat Mass Transfer 48 (2005) 2970–2985.
[31] C.B. Chiou, D.C. Lu, C.C. Chen, C.M. Chu, Heat transfer correlations of forced convective boiling for pure refrigerants in micro-fin tubes, Appl. Therm. Eng. 31 (2011) 820–826.
[32] J.F. Fa, W.K. Ding, J.F. Zhang, Y.L. He, W.Q. Tao, A performance evaluation plot of enhanced heat transfer techniques oriented to energy-saving, Int. J. Heat Mass Transfer 52 (2009) 33–44.
[33] L. Chamra, R. Webb, M. Randlett, Advanced microfin tubes for evaporation, Int. J. Heat Mass Transfer 39 (9) (1996) 1827–1838.